Investigation of T_e measurements discrepancies between ECE and Thomson diagnostics in high-performance plasmas in JET

M. Fontana[1,*], *G.* Giruzzi[2], *F. P.* Orsitto[3], *E.* de la Luna[4], *R.* Dumont[2], *L.* Figini[5], *D.* Kos[1], *M.* Maslov[1], *S.* Schmuck[5], *C.* Sozzi[5], *C. D.* Challis[1], *D.* Frigione[3], *J.* Garcia[2], *L.* Garzotti[1], *J.* Hobirk[6], *A.* Kappatou[6], *D.* Keeling[1], *E.* Lerche[7], *C.* Maggi[1], *J.* Mailloux[1], *F.* Rimini[1], *D.* Van Eester[1], and *JET contributors*[**]

[1]United Kingdom Atomic Energy Authority, Culham Centre for Fusion Energy, Culham Science Centre, Abingdon, Oxon, OX14 3DB, UK
[2]CEA, IRFM F-13108 Saint Paul-lez-Durance, France
[3]ENEA Department Fusion and Technology for Nuclear Safety, C R Frascati , 00044 Frascati, Italy
[4]National Fusion Laboratory, CIEMAT, Madrid, Spain
[5]Istituto per la Scienza e Tecnologia dei Plasmi, CNR, 20125 Milano, Italy
[6]Max-Planck-Institut für Plasmaphysik, D-85748 Garching, Germany
[7]Laboratory for Plasma Physics, LPP-ERM/KMS, Brussels, Belgium

Abstract. For high-temperature JET and TFTR discharges, electron cyclotron emission (ECE) measurements of central electron temperature were systematically found to be up to 20% higher than those taken with Thomson scattering. In recent high-performance JET discharges, central T_e measurements, performed with LIDAR Thomson scattering and the X-mode ECE interferometer, have been studied in a large database, including deuterium (DD), and deuterium-tritium plasmas (DT). Discrepancies between T_e measurements have been observed outside of the experimental uncertainties. ECE measurements, at high T_e, have been found to be higher or lower than those of LIDAR, depending on the specific plasma scenario. In addition, discrepancies between the peaks of the second and third harmonic ranges of the ECE spectrum have been interpreted as evidence for the presence of non-Maxwellian features in the electron distribution function. These comparisons seem to suggest that such features can be found in most of the high-performance scenarios selected in this JET database.

1 Introduction

Measurement of electron temperature (T_e) is one of the basic diagnostic requirements of any fusion experiment. Among the most common techniques used to evaluate T_e, are electron cyclotron emission (ECE) [1] and incoherent Thomson scattering (TS) [2], both of which have been widely employed in a variety of experiments for many decades. Despite the extensive experience operating these diagnostics and analysing the data they produce, it is known that values of T_e measured using ECE and TS can diverge substantially in some specific conditions. This was first observed on TFTR [3, 4] and on JET [5]. In pulses heated with neutral beam injection (NBI) and ion cyclotron resonance heating (ICRH), at high temperature (T_e>4-5 keV), it was found that ECE measurements of core T_e were systematically higher (up to 20%) than those taken using TS. In high T_e pulses at JET in 2004, ECE spectra in mainly extraordinary (X) mode polarisation showed higher second harmonic (X2) peak temperatures than the ones in the third harmonic (X3) range. At the same time, however, X3 peak temperatures showed good agreement with TS measurements [6]. But due to the high optical thickness (τ) of these plasmas in the third harmonic range and assuming a Maxwellian electron energy distribution function (EEDF), the two harmonics should match well. It has been proposed [7, 8] that the discrepancies between ECE and TS measurements, together with the anomalous ECE spectra, could be explained by a distortion of the EEDF in the bulk energy range, that is to say at energies close to the thermal energy of the core electrons. ECE and TS, in fact, operate based on different physical principles and respond differently to distortions of the EEDF. ECE measurements are particularly sensitive to the shape of the distribution function, with the absorption coefficient depending from the derivative of the EEDF [9]. To this point, no physical explanations for such EEDF distortions have been clearly identified yet. When a set of very similar experiments was repeated at JET in 2006, however, no discrepancy between ECE and TS, nor hints of non-maxwellian ECE spectra, were observed [6, 10]. A possible explanation was found in the higher hydrogen (H) concentration used in the 2006 pulses. In the intervening years, in fact, the lower limit of allowed hydrogen concentration at JET had been increased to reduce fast-ion losses that had been found to risk damage to the vessel

[*]e-mail: matteo.fontana@ukaea.uk
[**]See the author list of 'Overview of JET results for optimising ITER operation' by J. Mailloux et al. to be published in Nuclear Fusion Special issue: Overview and Summary Papers from the 28th Fusion Energy Conference (Nice, France, 10-15 May 2021)

walls. Higher H concentration affects the power distribution of ICRH between H and D ions and is believed to have reduced the temperature of the high-energy tail of the hydrogen ion distribution [6]. No more discrepancies between ECE and TS were observed in high-temperature (T_e up to 8 keV) experiments at JET from 2006 to 2018. Similar results were also obtained in experiments at Alcator C-mod. In plasmas heated with various configurations of ICRH, no discrepancy between ECE and TS was reported even though T_e up to 8 keV was reached [11]. From these experiments, it was concluded that these effects are not simply related to high electron temperatures, but must be influenced by other causes as well. Discrepancies between ECE and TS have instead been recently observed in very high-temperature (T_e up to 14 keV), EC heated pulses on FTU [12]. There, TS temperatures were found to greatly exceed ECE measured ones (up to 50% higher) in phases where T_e>8 keV, while they agreed inside the experimental uncertainty for lower temperatures.

The discrepancy between ECE and TS is extremely relevant for next-generation experiments such as ITER and future reactor-like devices. Accurate and consistent measurements of electron temperature are necessary both for physics studies and for the operation of a commercial facility. The fact that discrepancies between TS and ECE, supposedly two of the best understood and established diagnostic techniques in plasma physics, appeared in some of the most reactor-relevant experiments realized until now, including in the few experiments that used duterium-tritium (DT) mixtures, makes the problem even more important. In the past years, JET has worked to develop high-performance plasma scenarios after the installation of the ITER-like wall [13]. These efforts have culminated in the first experimental campaign using DT fuel since almost thirty years, which has marked a new record in generated fusion energy. This occasion presented an excellent opportunity to investigate the issue of ECE-TS discrepancies. For this, the core temperature measurements on JET have been collected in a large database, that covers different plasma conditions and isotopic compositions including DT plasmas. Study of this database highlighted different behaviours for various plasma scenarios. For T_e>5 keV, cases with $T_{e,ECE} > T_{e,TS}$ and with $T_{e,ECE} < T_{e,TS}$ have both been observed. Related ECE spectra seem to display features that could be attributed to the presence of EEDFs with non-Maxwellian characteristics.

Section 2 of this paper contains a description of the main diagnostics used to measure the core electron temperature at JET. Section 3 describes the criteria used to build the discharges database and the main characteristics of the scenarios to which the selected pulses belong. In Section 4, the observations based on the temperature measurements collected in the database are discussed. Finally, Section 5 summarizes the results and anticipates some of the work currently in progress.

2 Core T_e diagnostics at JET

Various choices are available for both ECE and Thomson diagnostics at JET. The standard ECE diagnostics available at JET are two Martin-Puplett interferometers [14] and one radiometer [15] observing the plasma through horizontal lines of sight, close to the vessel midplane (see Figure 1). The two interferometers collect radiation mainly of the ordinary (O) and extraordinary (X) wave mode, respectively. Both interferometers are absolutely calibrated, through the use of in-vessel sources over a wide spectral range (50-500 GHz). The temperature profiles (60 Hz acquisition frequency) can cover both low and high field side (LFS and HFS) of the tokamak (limited by harmonic overlapping for the X-mode) for the large range of the toroidal magnetic field available at JET (1.7-3.8 T). The spectral resolution is 3.66 GHz, corresponding to about 10 cm around the plasma axis. The 96-channels ECE radiometer is one of the main diagnostics used to study temperature fluctuations at JET, thanks to its high radial resolution (~2 cm) and acquisition frequency (from 5 to 200 kHz). The radiometer provides measurements on a range of frequencies that is changed pulse-by-pulse to follow to the plasma radial profile for X2 emission. Due to the different available configurations of mixers that can be selected to cover JET profiles at various magnetic field settings, the radiometer is cross-calibrated against the ECE interferometer on a pulse-by-pulse basis.

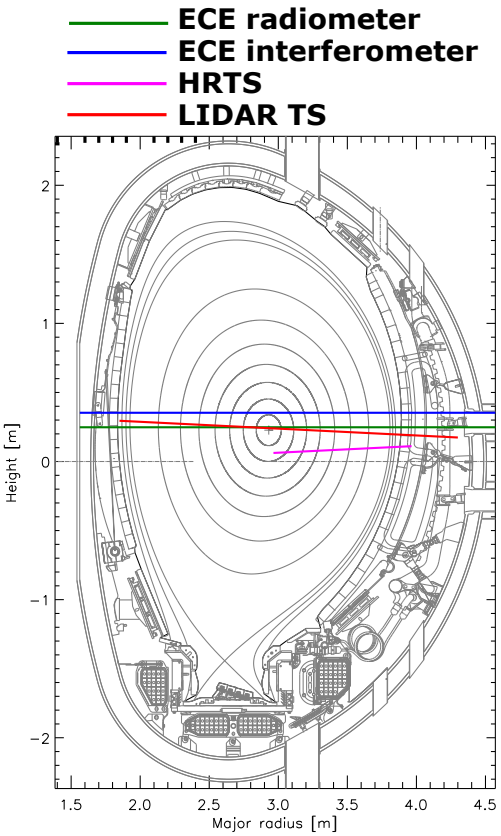

Figure 1: Lines of sight of the main electron temperature diagnostics on JET.

JET is also equipped with a high resolution Thomson scattering system (HRTS) [16, 17] and a LIDAR Thomson scattering diagnostic [18–20]. Both diagnostics are independently calibrated. LIDAR Thomson scattering pro-

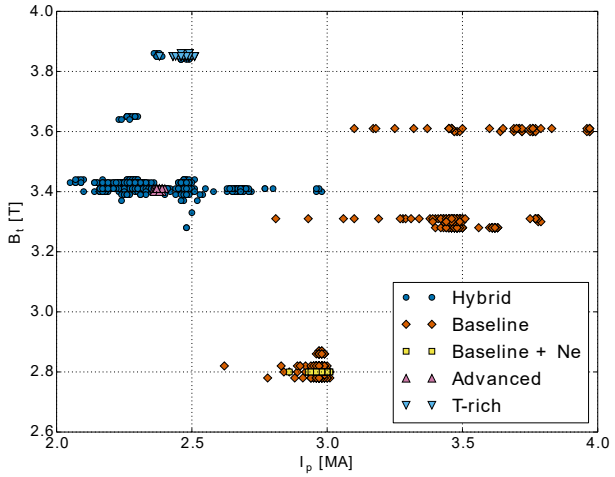

Figure 2: Plasma current (I_p) and toroidal field B_t of database points corresponding to flat-top phases for each pulse.

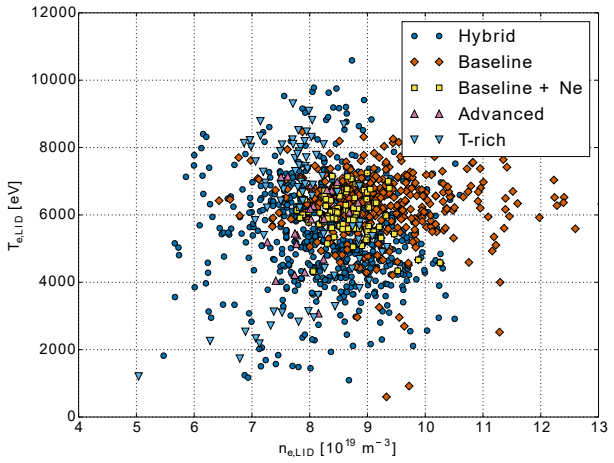

Figure 3: Electron density (n_e), and temperature (T_e) of database points corresponding to flat-top phases for each pulse.

vides density and temperature profiles covering the plasma LFS, core, and part of the HFS. The laser has a repetition frequency of 4 Hz, and every spatial point covers about 7 cm radially. HRTS provides better temporal (20 Hz) and spatial resolution (2 cm) compared with LIDAR. One of the main strenghts of HRTS is the excellent coverage of the plasma pedestal. However, as shown in figure 1, its line of sight is positioned slightly below the equatorial midplane of the JET vessel and is directly slightly downward. For this, in the majority of JET configurations, HRTS is limited to the LFS profile and does not manage to fully reach the plasma core, usually stopping at ρ>0.2 in normalized radial coordinates. Since the effects described in this work have been mostly observed in proximity to the plasma axis, HRTS was excluded from the analysis.

Also measurements from the ECE radiometer have not been included in this study. Due to the relatively low repetition rate of LIDAR, in fact, the high temporal resolution of the ECE radiometer is not necessary for comparing the two techniques. Furthermore, the radiometer does not allow comparison of second and third harmonics. In conclusion, the diagnostics that will be referred to in the rest of the paper for ECE and TS measurement are the X-mode ECE interferometer and the LIDAR Thomson scattering system respectively.

3 Pulse selection for the database

ECE and TS measurements have been compared for pulses from several JET campaigns from 2018 to 2022. These experiments include DD and DT plasmas covering a variety of high-performance plasma scenarios, designed to demonstrate high fusion power for about five seconds with the ITER-like wall. The two main ones are the so-called baseline and hybrid scenarios. The baseline scenario employs high field (2.8-3.5 T), high current (3-4 MA) and high density (7-11 $\times 10^{19} m^{-3}$ in the core), using pellet injection to control edge localised modes. The goal is to reach stable, high-performance conditions similar as to what is foreseen for the standard ITER scenario [21]. Some DD pulses in this category included various levels of Ne seeding to improve confinement through controlled edge radiation. Hybrid pulses work at high field (3-3.9 T) but lower current (2-2.8 MA) compared to baseline ones, aiming for high β operation. The particular current profile developed for these pulses ($q_{95} > 3$, $q_0 \geq 1$) strongly reduces the occurrence of deleterious MHD modes in the plasma flat-top phase [22]. During the DT experiments, some of these pulses were designed to optimize non-thermal fusion reactions, with T-rich plasmas heated by D-only NBI. Finally, the database also includes pulses belonging to experiments exploring advanced scenarios, studying internal transport barriers, energetic particle modes and afterglow [23].

For each pulse, LIDAR times were selected where the laser energy was above 0.4 J and T_e>1 keV. For each of these points, the closest ECE time, with a maximum difference of 10 ms, was identified. ECE spectra were converted into radial profiles using a magnetic reconstruction based only on magnetic measurements with no further constraints. For each ECE and LIDAR T_e radial profile, a representative value of the centre is determined by averaging the measurement points included between 2.85-3.15 m. This averaging window helps to smooth out the effects of the different lines of sight for the two diagnostics (see Figure 1) and the uncertainties in the localization of the plasma axis position. The values used to compare the second and third harmonics of the ECE spectra were calculated averaging T_e in the interval +/- 5% around the frequency corresponding to the plasma centre according to the equilibrium reconstruction.

The points that make up the database cover the evolution of the pulses from ramp-up to ramp-down or disruption. During the flat top phase for these pulses, the combinations of toroidal magnetic field (B_t), plasma current (I_p) and electron density (n_e) and temperature (T_e) covered by the different scenarios are shown in Figures 2 and 3 re-

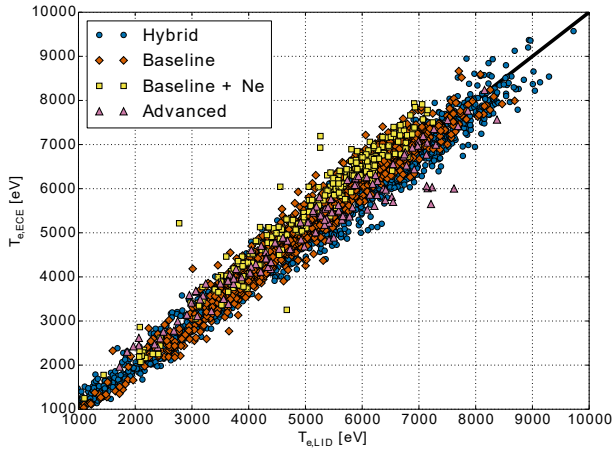

Figure 4: Comparison of central ECE and LIDAR temperatures in DD pulses.

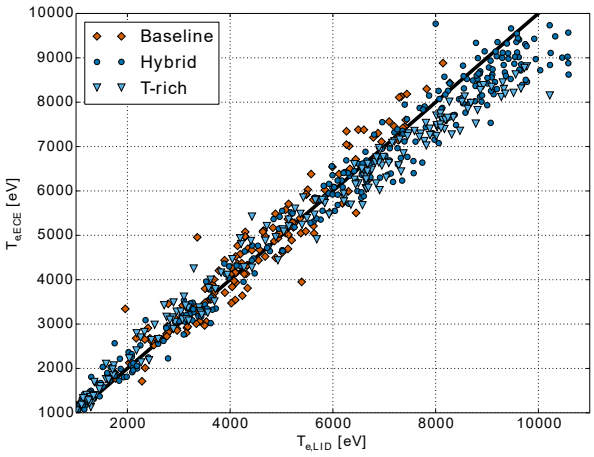

Figure 5: Comparison of central ECE and LIDAR temperatures for DT pulses.

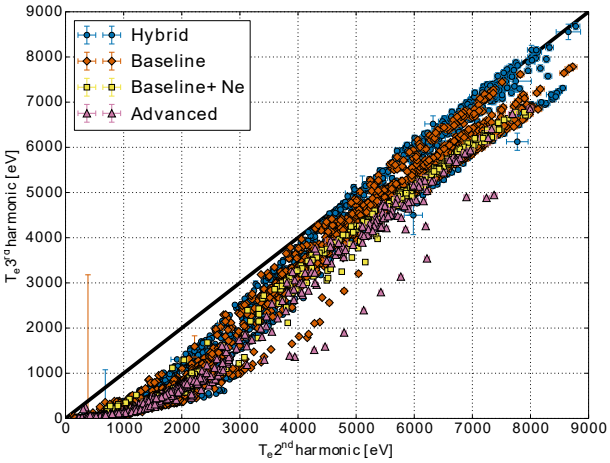

Figure 6: Comparison of peak temperatures for second and third harmonics X-mode in DD pulses.

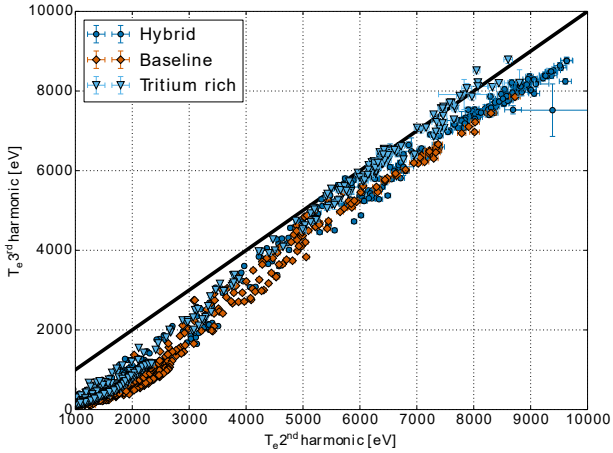

Figure 7: Comparison of peak temperatures for second and third harmonics X-mode in DD pulses.

spectively. Each point corresponds to a LIDAR time included in the database. These pulses were heated via NBI and/or ICRH. The maximum heating power reached was 38.5 MW, in some of the hybrid pulses. In the following, only pulses with $T_e > 5$ keV in the core will be discussed.

4 Discussion

The central averages of T_e for LIDAR and ECE, calculated as detailed in Section 3, have been compared, separating DD pulses from DT pulses. For the DD pulses, in Figure 4, $T_{e,ECE}$ and $T_{e,LID}$ are quite similar for most pulses. However, it is possible to distinguish significant differences comparing the different scenarios. Baseline pulses with Ne seeding, in particular, appear to have $T_{e,ECE} > T_{e,LID}$, similar to what was observed in past experiments at JET and TFTR [4, 5], even though to a lower extent. A clear difference is visible between these baseline pulses and those with no Ne seeding, and even more when they are compared with the hybrid pulses. A similar situation can be observed for DT pulses in figure 5. Here the largest discrepancies ($T_{e,LID} > T_{e,ECE}$) are observed for hybrid pulses, and especially T-rich experiments, while baseline pulses tend to remain closer to $T_{e,LID} = T_{e,ECE}$.

The discrepancies between $T_{e,LID}$ and $T_{e,ECE}$ have been suggested to be related to the presence of non-Maxwellian features in the EEDF [7]. This explanation is consistent with the higher X2 peak temperature, compared with X3 and Thomson scattering diagnostics, observed for some of these pulses. In figure 6, we can observe that, as expected, for low T_e, X3 peak temperature is consistently lower compared with X2. This is due to the low τ_{X3} at these points. With increasing temperature, however, τ_{X3} increases and, in presence of a Maxwellian EEDF, $T_{e,X3}$ should approach $T_{e,X2}$. In this case this seems to happen only for a fraction of the baseline and hybrid pulses while, in the rest of the points, $T_{e,X3}$ remains consistently below $T_{e,X2}$ even at very high T_e. Also for the DT pulses, only some pulses display $T_{e,X3} \sim T_{e,X2}$, as shown in Figure 7. In this case however, the different scenarios remain rather well separated. In particular the T-rich pulses display the best agreement between second and third harmonic at high T_e. This increased uniformity in each scenario is due to

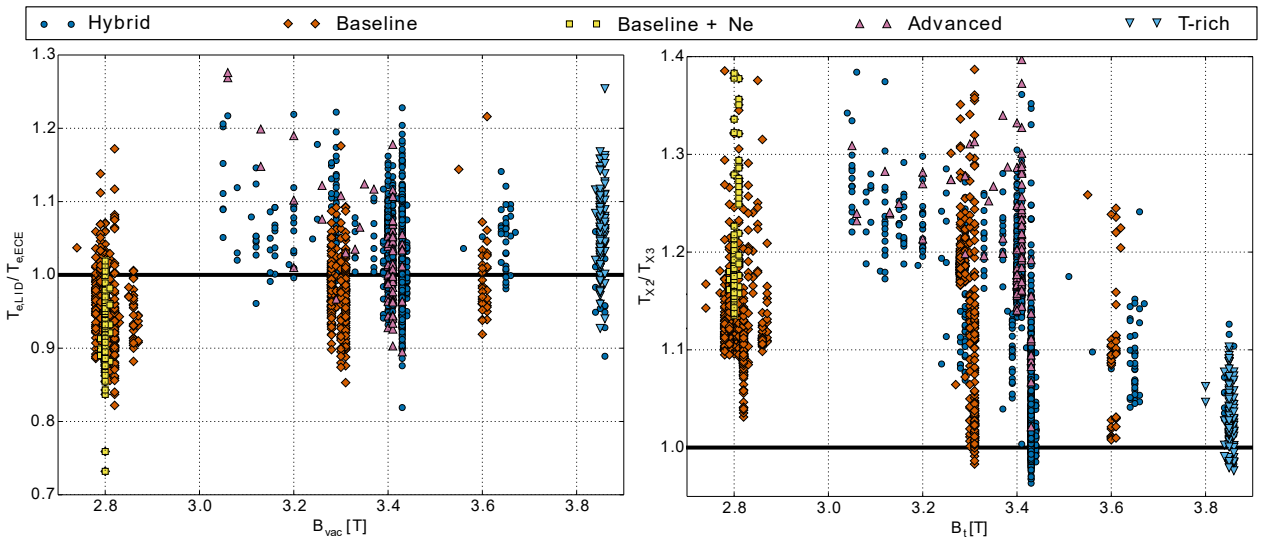

Figure 8: Ratio of ECE and LIDAR measurements (a) and ratio between the peaks of X2 and X3 emission (b) as a function of the vacuum magnetic field B_{vac}.

the fact that almost no time was dedicated to scenario development in the DT campaign, in order to minimize the consumption of nuclear fuel and neutron budget. As a consequence, the parameters of each discharge changed little for a given scenario.

A possible explanation for $T_{e,X3} < T_{e,X2}$ that does not imply the existence of non-Maxwellian features in the EEDF, is the presence of errors in the calibration of the ECE interferometer, in particular affecting the comparison of second and third harmonics. In this case, different ratios of $T_{e,X3}/T_{e,X2}$ would be related only to changes in the magnitude of the magnetic field of the various pulses. While no in-vessel calibrations have been possible since 2018, the properties of the instruments were constantly monitored regularly repeating in-lab measurements on a cold (liquid N_2) and a room temperature source. These measurements have been used to correct for changing sensitivity of the diagnostic, greatly improving agreement of the ECE profiles with those produced by LIDAR and HRTS. Concerning the measurements in this database, Figure 8a shows that the ratio between LIDAR and ECE measurements (limited to $T_{LID} > 4keV$) is not correlated with the vacuum magnetic field (B_{vac}). Figure 8b, instead, shows the ratio between second and third harmonics against B_{vac}. Here, it can be observed that, while most of the points for baseline pulses that reach $T_{X3} \sim T_{X2}$ are concentrated at B_{vac} ~3.3 T and higher, similar examples can be found also for cases around ~2.8 T.

5 Conclusions and prospects

A very large database of T_e measurements (more than 14000 time points from 246 discharges) was collected from high performance DD and DT pulses performed at JET. These include a variety of plasma conditions and different scenarios, some of which were tested using DT mixture for the first time. These measurements, taken with LIDAR Thomson scattering and an X-mode interferometer, showed discrepancies when high T_e were reached. Differently from what had been observed in the previous studies of this kind [3–5], here the discrepancies were less pronounced and, most importantly, they were not only in the direction of $T_{ECE} > T_{LID}$ for high T_e. In fact, a richer phenomenology was observed, including also $T_{ECE} < T_{LID}$, with different scenarios showing different behaviours. Comparison of the peaks of the second and third harmonics of the ECE spectra suggests the presence of non-Maxwellian features of the EEDF for most of the pulses in this data set. Even for plasma conditions where τ_{X3} was large enough to have $T_{X2} \sim T_{X3}$, in fact, $T_{X2} > T_{X3}$ was observed instead in many pulses.

The possibility that EDF distortions could result in different measurements from ECE and Thomson diagnostics can be investigated using simple models that applies an arbitrary perturbation in velocity space to a Maxwellian EEDF and then calculating the resulting ECE spectrum. Such a study, employing a bipolar distortion of a Maxwellian EEDF, comparing the results of the model with the experimental measurements presented in this database, obtained promising results [24]. However, at the moment, a clear physical cause for EDF distortions which could give rise to these discrepancies has not yet been identified. Several hypothesis have been suggested and are being investigated, including, for example, effects related to the fast ion population (high NBI/ICRH power and DT fusion reactions). The ions could interact with the electron population directly through collisions or through the excitation of MHD modes (such as Alfvén modes) that can then transfer energy to the electrons. The latter possibility is being investigated via gyrokinetic simulations for parameters approaching those of some cases included in the database. The database presented in this work could be further expanded by the inclusion of other diagnostics. For example, equilibrium reconstructions that included con-

straints from more sources (such as ion and electron temperature and density) would allow better comparisons between diagnostics with different lines of sight, such as HRTS. Furthermore, data from the second ECE interferometer on JET, collecting emission predominantly in O-mode will be added to the database to study also O1 emission. Finally, JET is equipped with an oblique ECE system which collected data for some of the pulses included in this work. Processing these data could result in another way to obtain information on the EEDF.

6 Acknowledgements

This work has been carried out within the framework of the EUROfusion Consortium, funded by the European Union via the Euratom Research and Training Programme (Grant Agreement No 101052200 — EUROfusion). Views and opinions expressed are however those of the author(s) only and do not necessarily reflect those of the European Union or the European Commission. Neither the European Union nor the European Commission can be held responsible for them. This work has been part-funded by the EPSRC Energy Programme [grant number EP/W006839/1]. To obtain further information on the data and models underlying this paper please contact PublicationsManager@ukaea.uk. For the purpose of open access, the authors have applied a Creative Commons Attribution (CC BY) licence to any Author Accepted Manuscript version arising.

References

[1] A.E. Costley, R.J. Hastie, J.W.M. Paul, J. Chamberlain, Phys. Rev. Lett. **33**, 758 (1974)

[2] J. Sheffield, in *Plasma Scattering of Electromagnetic Radiation*, edited by J. Sheffield (Academic Press, 1975), pp. 191–210, ISBN 978-0-12-638750-6, https://www.sciencedirect.com/science/article/pii/B9780126387506500148

[3] I. Fidone, G. Giruzzi, G. Taylor, Physics of Plasmas **3**, 2331 (1996)

[4] G. Taylor, R.W. Harvey, Fusion Science and Technology **55**, 64 (2009), publisher: Taylor & Francis _eprint: https://doi.org/10.13182/FST55-64

[5] E. de la Luna, V. Krivenski, G. Giruzzi, C. Gowers, R. Prentice, J.M. Travere, M. Zerbini, Review of Scientific Instruments **74**, 1414 (2003)

[6] E. De La Luna, D. Farina, L. Figini, G. Grosseti, S. Nowak, C. Sozzi, M. Beurskens, O. Ford, T. Johnson, E.c. Jet, in *Electron Cyclotron Emission and Electron Cyclotron Resonance Heating (EC-15)* (WORLD SCIENTIFIC, 2009), pp. 200–207, ISBN 978-981-281-463-0, https://www.worldscientific.com/doi/10.1142/9789812814647_0026

[7] V. Krivenski, Fusion Engineering and Design **53**, 23 (2001)

[8] V. Krivenski, 29th EPS Conf. on Plasma Physics, ECA **26B** (2002)

[9] G. Giruzzi, Nucl. Fusion **28**, 1413 (1988), publisher: IOP Publishing

[10] K.V. Beausang, S.L. Prunty, R. Scannell, M.N. Beurskens, M.J. Walsh, E. de La Luna, Review of Scientific Instruments **82**, 033514 (2011), publisher: American Institute of Physics

[11] A.E. White, A.E. Hubbard, J.W. Hughes, P.T. Bonoli, M.E. Austin, A. Bader, R.W. Harvey, Y. Lin, Y. Ma, M.L. Reinke et al., Nucl. Fusion **52**, 063021 (2012), publisher: IOP Publishing

[12] G. Pucella, E. Alessi, S. Almaviva, B. Angelini, M.L. Apicella, G. Apruzzese, M. Aquilini, G. Artaserse, B. Baiocchi, M. Baruzzo et al., Nucl. Fusion **62**, 042004 (2022), publisher: IOP Publishing

[13] F. Romanelli, Nucl. Fusion **53**, 104002 (2013), publisher: IOP Publishing

[14] S. Schmuck, J. Fessey, J.E. Boom, L. Meneses, P. Abreu, E. Belonohy, I. Lupelli, Review of Scientific Instruments **87**, 093506 (2016)

[15] E. de la Luna, J. Sánchez, V. Tribaldos, E.c. Jet, G. Conway, W. Suttrop, J. Fessey, R. Prentice, C. Gowers, J.M. Chareau, Review of Scientific Instruments **75**, 3831 (2004), publisher: American Institute of Physics

[16] R. Pasqualotto, P. Nielsen, C. Gowers, M. Beurskens, M. Kempenaars, T. Carlstrom, D. Johnson, Review of Scientific Instruments **75**, 3891 (2004)

[17] L. Frassinetti, M.N.A. Beurskens, R. Scannell, T.H. Osborne, J. Flanagan, M. Kempenaars, M. Maslov, R. Pasqualotto, M. Walsh, Review of Scientific Instruments **83**, 013506 (2012)

[18] H. Salzmann, K. Hirsch, Review of Scientific Instruments **55**, 457 (1984), publisher: American Institute of Physics

[19] H. Salzmann, J. Bundgaard, A. Gadd, C. Gowers, K.B. Hansen, K. Hirsch, P. Nielsen, K. Reed, C. Schrödter, K. Weisberg, Review of Scientific Instruments **59**, 1451 (1988), publisher: American Institute of Physics

[20] M. Maslov, M.N.A. Beurskens, M. Kempenaars, J. Flanagan, J. Inst. **8**, C11009 (2013), publisher: IOP Publishing

[21] L. Garzotti, C. Challis, R. Dumont, D. Frigione, J. Graves, E. Lerche, J. Mailloux, M. Mantsinen, F. Rimini, F. Casson et al., Nucl. Fusion **59**, 076037 (2019), publisher: IOP Publishing

[22] J. Hobirk, F. Imbeaux, F. Crisanti, P. Buratti, C.D. Challis, E. Joffrin, B. Alper, Y. Andrew, P. Beaumont, M. Beurskens et al., Plasma Phys. Control. Fusion **54**, 095001 (2012)

[23] R.J. Dumont, J. Mailloux, V. Aslanyan, M. Baruzzo, C.D. Challis, I. Coffey, A. Czarnecka, E. Delabie, J. Eriksson, J. Faustin et al., Nucl. Fusion **58**, 082005 (2018), publisher: IOP Publishing

[24] G. Giruzzi, M. Fontana, F.P. Orsitto, E. De La Luna, R. Dumont, L. Figini, M. Maslov, S. Mazzi, S. Schmuck, L. Senni et al., This workshop (2022)